

NOVEL TECHNIQUES FOR SLURRY BUBBLE COLUMN HYDRODYNAMICS

FIRST ANNUAL REPORT FOR GRANT DE-FG 22-95-PC 95212

July 1, 1996

**SECTION V: REPORT FROM EXXON RESEARCH AND ENGINEERING
ON JOINT WORK WITH WASHINGTON UNIVERSITY IN
PREPARATION FOR HIGH PRESSURE MEASUREMENTS**

Min Chang
Exxon Research and Engineering
PO Box 101
Florham Park, NJ 07932
FAX: 201-765-1189
E-mail: mchang@crsgil.erenj.com

with

Jinwen Chen, Puneet Gupta, Sailesh Kumar
Chemical Reaction Engineering Laboratory
Washington University
Department of Chemical Engineering
One Brookings Drive
St. Louis, Missouri 63130

Computation of Particle Source Strength for CARPT Experiment

Following are the details for the basis of computing the source strength of the radioactive particle required for the CARPT experiment, given the column size, material of construction and physical properties of the two or three phase system to be studied.

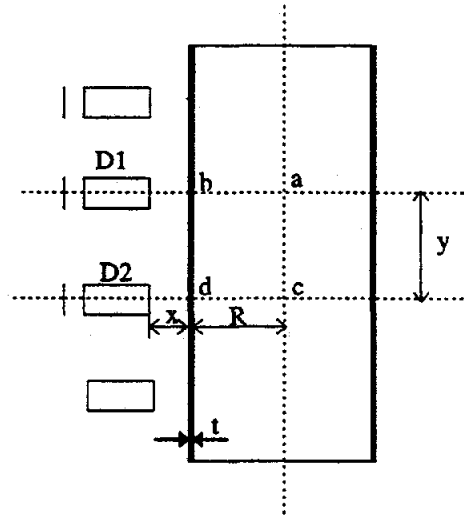


Figure 1 : Schematics of the detector setup for CARPT

For a given detector spacing, y , the lowest count rate for a given detector, say D1, would be obtained if the radioactive tracer particle was located half-way between points a & c (Fig. 1), and the maximum count rate would be obtained if the radioactive particle was in position b , or d for detector D2. For the CARPT data to be reasonable for reconstruction of a calibration map for future identification of particle position, a conservative estimate on the lowest count rate is 1500 photons/sec. Also, saturation of the detectors limits the maximum count rate to no more than 12000 photons/sec (again a slightly conservative estimate). These two constraints provide the bounds for the source strength of the radioactive particle that has to be used. The variable x is the distance of the detectors from the outer wall of the reactor, and is equal to zero if the detectors are flush mounted. At the worst location of the particle in the reactor, we would like to have a count rate of 1500 or more, and at the best location of the particle, we would want a count rate of 12000 or less. Keeping these in mind, an optimization problem could be set up to minimize the source strength requirements, with the distance of the detector from the reactor wall being an additional manipulated variable. Figures 2a and 2b show the different geometrical quantities to be estimated for the calculation of the attenuation factor (A.F.) and the solid angle (Ω) for the best and worst locations of the tracer particle, respectively. The following is the governing equation for the calculation of the count rate at a given detector.

$$CR = [(A.F.) (B.F.) v S \varepsilon \Omega] / f \quad (1)$$

where,

- f = sampling frequency, Hz
- A.F. = attenuation factor
- B.F. = build-up factor
- Ω = solid angle
- ε = detector efficiency
- CR = count rate
- S = particle source strength, Bq
- v = # of photons γ per disintegration, approximately equal to 2 for Co^{60} and Sc^{46}

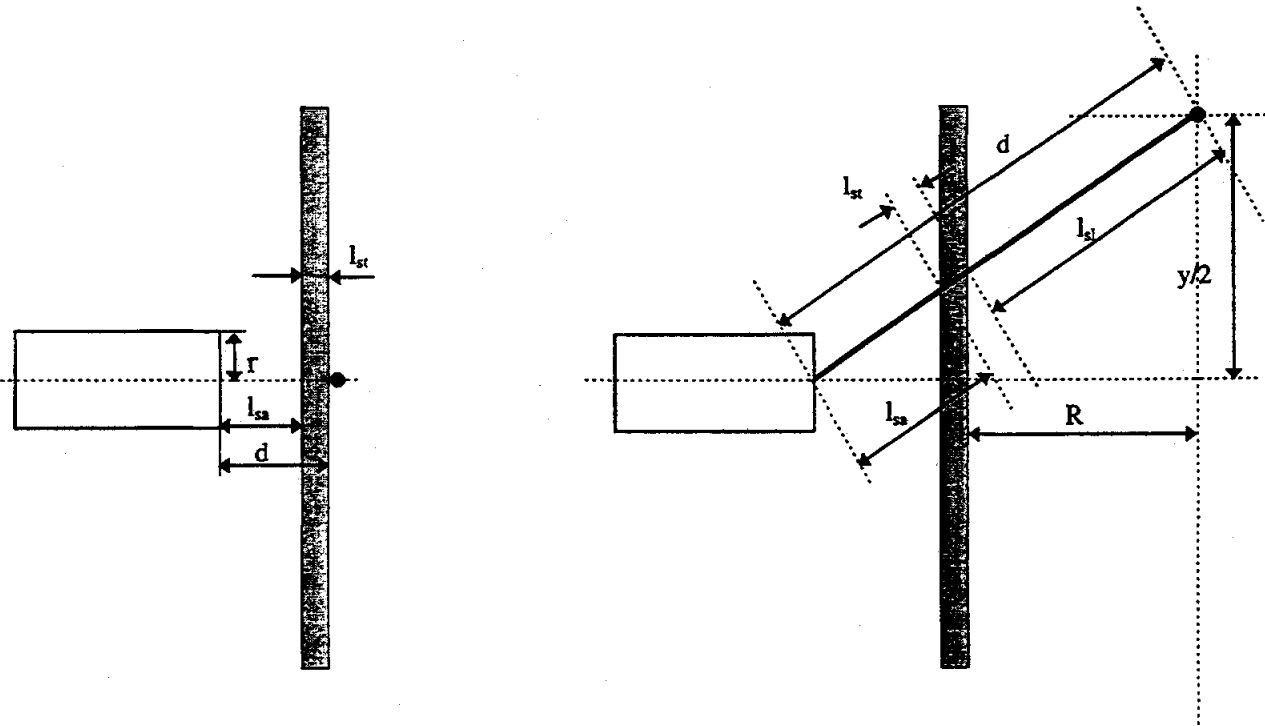


Figure 2a : Particle at best location.

Figure 2b : Particle at worst location

In Figures 2a and 2b, r is the radius of the detector face, R is the radius of the reactor, t is the thickness of the reactor wall, d is the total path length of the radiation before being intercepted by the detector, l_{sa} is the path length through air, l_{st} is the path length through the material of the column wall, and l_{sl} is the path length through the multiphase medium.

The build-up factor (B.F.) and the efficiency of the detectors are to be chosen with some prior experience with the attenuation through the reactor wall material, whereas, the attenuation factor (A.F.) and the solid angle can be computed from the following relations.

The optimization problem could now be setup as described below :

Minimize S (13)

subject to the following constraints

$$S \geq 0$$

$$X \geq x \geq 0$$

$$(\text{CR})_{\text{Case I}} \leq 12,000$$

$$(\text{CR})_{\text{Case II}} \geq 1,500$$

where,

X = the maximum allowable distance of the detector face from the reactor wall (usually not more than an inch and a half).

(CR)_{Case I} = count rate when particle is in a position as given in Figure 2a.

(CR)_{Case II} = count rate when particle is in a position as given in Figure 2b.

This optimization could be carried out using the "MATLAB Optimization Toolbox". The routine was run for the following cases pertinent to the Exxon column.

Table 1 : Physical Properties.

Parameter	Value [units]
μ_{sa} [Sc ⁴⁶]	0.0674405 [cm ² /gm]
μ_{st} [Sc ⁴⁶]	0.0639 [cm ² /gm]
μ_{sl} [Sc ⁴⁶]	0.0726 [cm ² /gm]
μ_{water} [Sc ⁴⁶]	0.0749 [cm ² /gm]
μ_{sa} [Co ⁶⁰]	0.0594172 [cm ² /gm]
μ_{st} [Co ⁶⁰]	0.0561 [cm ² /gm]
μ_{sl} [Co ⁶⁰]	0.0640 [cm ² /gm]
μ_{water} [Co ⁶⁰]	0.0661 [cm ² /gm]
ρ_{water}	1.0 [gm/cm ³]
ρ_{sa}	1.2884 x 10 ⁻³ [gm/cm ³]
ρ_{st}	7.762 [gm/cm ³]
ρ_{sl}	1.45 [gm/cm ³]
r	2.75 [cm]
t	0.28 [inches]
R	3.025 [inches]

The results from the optimization procedure are as follows :

Detector level spacing, $\gamma = \pm 6.0$ inches, $X = 1.0$ inches

Radioactive Nuclide	Source Strength for slurry system [μCi]	Source Strength for Gas-Liquid system [μCi]	x [inches]
Co ⁶⁰	328	248	0
Sc ⁴⁶	395	288	0

Detector level spacing, $\gamma = \pm 12.0$ inches, $X = 1.0$ inches

Radioactive Nuclide	Source Strength for slurry system [μCi]	Source Strength for Gas-Liquid system [μCi]	x [inches]
Co ⁶⁰	1267	891	1
Sc ⁴⁶	1607	1077	1

Detector level spacing, $\gamma = \pm 12.0$ inches, $X = 0.5$ inches

Radioactive Nuclide	Source Strength for slurry system [μCi]	Source Strength for Gas-Liquid system [μCi]	x [inches]
Co ⁶⁰	1371	935	0.5
Sc ⁴⁶	1777	1149	0.5

For the above cases, the B.F.F. was taken as 2.5 and ϵ was taken as 0.35. These have been chosen after some experimental validation on a 7 mm thick steel pipe in our laboratory with a particle source strength of 400 μCi . These calculations thus provide the first basis for calculating the required source strengths, and since there are no strict guidelines to estimate the build-up factor r and the detector efficiencies, some arbitrariness could not be avoided. More sophisticated techniques like Monte Carlo could be used to calculate the detector efficiencies and solid angles subtended by the detector, for particular particle locations inside the reactor, to greater accuracy. But the effort involved in their implementation may not yield significant improvements in predicting source strengths for particular applications.

Thus, we see that for the experiments to be conducted at Exxon, a Sc⁴⁶ particle of source strength of 400 μCi would suffice.

The Design of Calibration Device for the High Pressure System

1. Introduction

The high pressure slurry bubble column reactor at EXXON is made of stainless steel. The present method of calibration, which uses fishing lines and hooks to position the radioactive particle, will not work because the column is not transparent. Thus a different calibration device should be designed and constructed. While the present fishing line-hook method is very time consuming and labor intensive, as known to all the members of CREL, a method based on Monte Carlo simulation is currently being developed to dramatically reduce the time required for calibration. In addition, an automatically controlled positioning device would be best to perform the calibration at EXXON. Such a device is a feasible alternative for the present calibration method in CREL, and may be called the third generation of calibration device. (The first generation of calibration device used a long rod connected by four short rods, the particle is fixed at the tip of the bottom rod, the other end of the rod is fixed on a rotating support to achieve different axial and azimuthal positions in the column. The problem of this device is that when the column is high, say higher than 6 feet, or the flow in the column is very turbulent, the positioning of the particle becomes difficult because of the vibration of the rod caused by the flow in the column. The second generation of the calibration device is the present one, fishing line-hook method, which is time consuming and labor intensive. Another problem of the present method is that if there is something wrong during the calibration, for example, the tangling and breaking of the lines, one will have to do the calibration from beginning because the detectors have to be removed and repositioned again in order to open the column. For stainless steel column, marking the lines will be more difficult and by no means one can check the positioning of the particle by matching the marks on the lines)

2. Description of the device

With the above ideas in mind, a preliminary configuration of a new calibration device is proposed and a draft drawing is presented (please see the attached drawings). The feasibility of the mechanics of the system and machining of the proposed design has been discussed among the EXXODN project members as well as some mechanics in Washington University (Mr. Harkins, the Engineering School; Mr. Krietler, the Medical school and Mr. James, the Art and Science School).

The design consists of the following parts:

1. Two supports made of four 3/8" tubes(1) (see Figure 1 and Figure 3) . One end of the tubes is screwed into a cross-shaped support to make the whole support more rigid as well as to be able to adjust the length of the tube to match the column diameter. One of the tubes is used to support the particle-holding rod and is made in such a way that the rod position can be varied to get different radial positions in the column. There is a ball fixed at the ends of the four tubes. The balls rotate in any direction to ensure that the supports can move up and down and also rotate in the azimuthal direction. Attached to the two adjacent balls of the four, which are not on the tube to support the particle-holding rod, is a spring, the other end of which is fixed on the tube. The springs are under tension so that they always push the attached ball against the inner wall of the column and so that the ball can rotate smoothly in any direction. On the end of the other two tubes, a ball of the same size is fixed with no spring. Such a structure is designed to make the whole support more stable and to reduce the time of vibration after the device move to a new position. The balls must be of the same size and the springs must have the same tension. Some small holes are drilled in the tubes to let the water in the tube flow out when the calibration is being performed . Two piece of supports are fixed on one end of the first measuring rod with a distance of about 1 foot to ensure that the whole device moves vertically without any slanting. In addition, a small bar (1/4" diameter) is fixed vertically between the two supports to make them more stable. Also the particle-holding rod is designed to be able to be

fixed either on both of the supports to prevent it from vibrating when there is a turbulent flow in the column or only on the bottom support.

2. Measuring rods(2) (see Figure 3). The measuring rods are five pieces of square bars (which are connected together with screws if head space is limited). Three of them are 2 feet long and the other two 1 foot long. Scales are made on one side of the rod for visual measurement. On the opposite side of the rod, a gear belt is fixed with which a step motor can be used to drive the rod up and down. It is essential that the gears of the belts exactly coincide in the joint when the two rods are connected together so that the step motor can drive the whole device smoothly.
3. Step motors(3 and 4) (see Figure 1 and Figure 2). Two step motors are used, one of which(4) drives the device up and down to different axial positions, while the other one(3) rotates the device to different azimuthal positions at a given radial position. It should be pointed out here that one has to change the radial position manually by fixing the particle support rod(5) at different radial positions on the two supports (or the bottom support). The two step motors (including the corresponding gears), are supported on a plate which is fixed on a separated flange connected with the top flange of the column. On the support plate some round windows are opened to let air out of the column when the system is running. For a given calibration, the axial position is set first. After finishing taking data at all azimuthal positions of the same plane, a new axial position is set (the axial positions are set from bottom to top). After finishing all the axial and azimuthal positions for a given radial position, a new radial position is set manually and axial and azimuthal calibration is repeated. Only 3 to 5 radial positions are needed.
4. Some kind of lock is needed to prevent the measuring rod from dropping down when the system is running (in case), which may cause the cracking of the radioactive particle. A simple way to do this is that connecting a flexible steel rope to the top support, while the other end of the steel rope is fixed at somewhere of the top of the column. A maximum tolerable length is given to stop the device before it drop down to the bottom of the column.

3.0 Procedure and cost estimation

The cost for making the device has been estimated by the machine shop personnel on campus as follows:

Manual control for 6" column: \$ ~ 1500.00 ~ 2000.00

Step motor control for 6" column: \$ ~ 4500.00

Extend to 4", 8", 12", 18" columns : \$ ~ 5500.00

Since this is a big project, it would be reasonable to start with manual control for a 6" column (such as the one at EEXXON), to verify the feasibility of the proposed design and make some modifications if necessary. Next we will try to use the step motor control, automate the system and finally extend it to other columns.

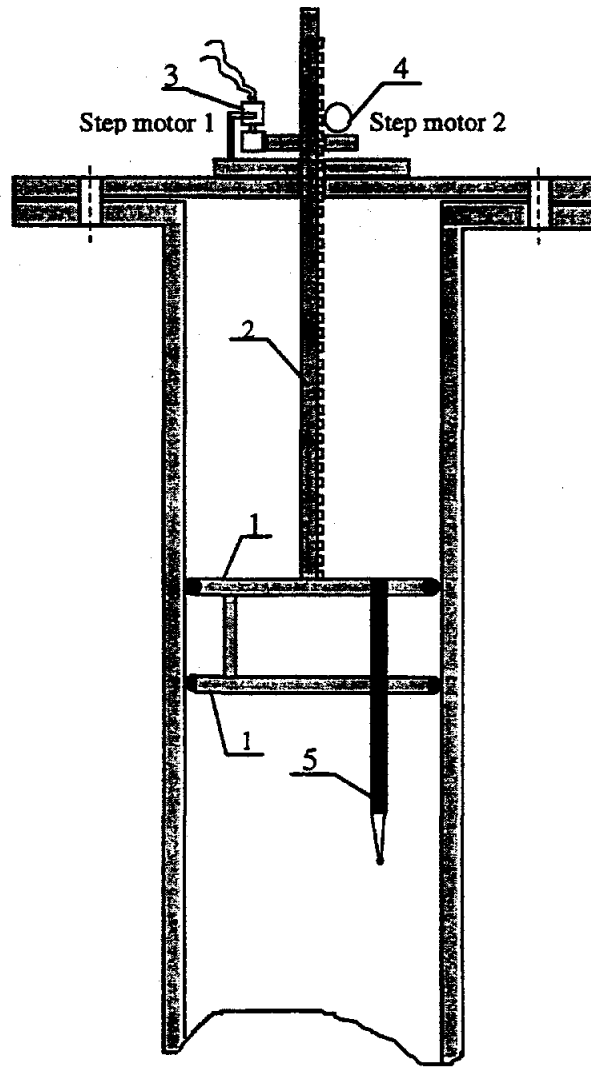


Figure 1. Overall Configuration of the Calibration Device

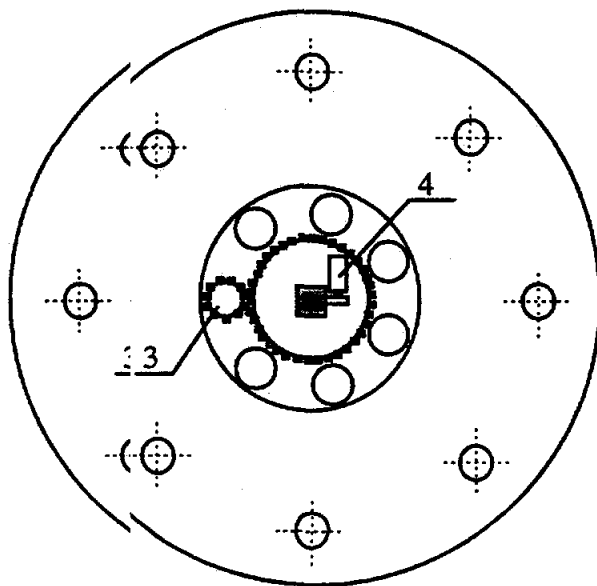


Figure 2. Top View of the Calibration Device

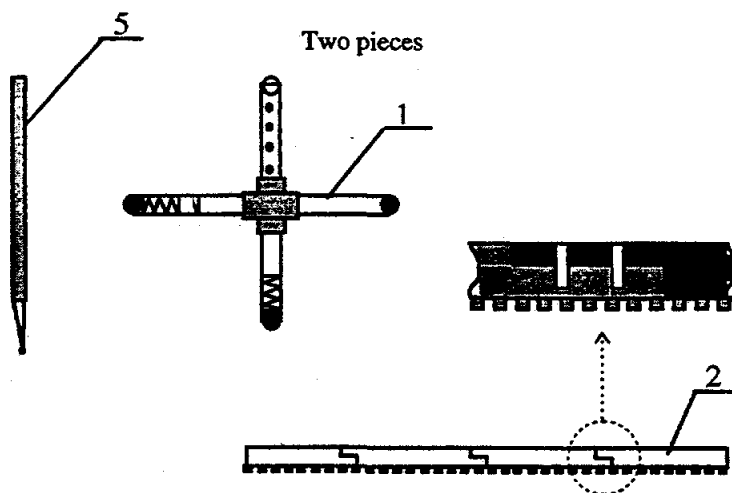


Figure 3. Details of the Support, Particle-holding Rod and Measuring Rod

Computational Fluid Dynamics Case Studies (Simulation of a Two Dimensional Bubble Column)

For this simulation the experimental condition of interest is the two dimensional bubble column studied by Dr. Fan's group at the Ohio State University. The column has a width of 48.3 cm and a height of 160.0 cm. The gas distribution is by means of 0.0016 cm diameter injectors, although the number of injectors used is not clear. For this simulation the gas is assumed to be distributed uniformly across the column width. Measurements of the velocity and gas holdup profiles at different axial positions obtained using Particle Image Velocimetry have been reported (Lin et al., 1996). The figure for the experimental results at a superficial gas velocity of 3.34 cm/s (from their manuscript) is enclosed as Figure 1. The time averaged axial liquid velocity and gas holdup profiles at different axial positions are shown in Figure 1. The quantity L_m / L_s in the figure represents the ratio of the measuring point height to the static liquid height.

The simulation was performed in two dimensional planar coordinates, with the no slip boundary condition at the walls, inflow of gas at the bottom of the domain and pressure set to a reference value (atmospheric) at the free surface. Since the static liquid height has not been specified, the initial liquid height for the simulation was adjusted to ensure that the expanded height of the dispersion fills the available column height of 160.0 cm. In a two dimensional geometry as the present one, CFD simulations normally indicate the presence of a series of circulation cells along the axis of the column. This has also been observed experimentally by Chen et al., 1989, and is also consistent with the flow structure proposed by Dr. Fan's group. These circulation cells persist in the flow pattern even after time averaging.

For obtaining a flow field in a two dimensional column which shows the presence of circulation cells, such as those observed by Chen et al. (1989), the values for some parameters of the interfacial momentum exchange have been standardized for CFDLIB codes. These include a bubble size of 0.5 cm, a lift coefficient of 0.1 and a turbulence length scale about 0.5 to 1.5 cm (with column width ranging from 10 to 50 cm). For the present case a mixing length of 1.0 cm was used and the coefficient of virtual mass was set to 0.5 following standard practice. The first simulation attempt did show the presence of persistent circulation cells. However, with such a flow field the time averaged velocity profiles are different from the results reported by the Dr. Fan's group and are shown in Figure 2. The interval for time averaging was from 25 to 100 seconds. The downward axial liquid velocities are much larger than reported PIV values and the presence of the circulation cells gets reflected in the large magnitude of the radial velocities.

The PIV experimental results for the time averaged velocity and gas holdup profiles re-

ported (Figure 1) are more consistent with a flow structure that does not show the circulation cells after time averaging. To be able to obtain the velocity and holdup profiles reported experimentally the mixing length scale had to be increased to 1.8 cm and the pressure of the two phases had to be made significantly different. All other parameters in the models for interfacial momentum exchange were identical to the ones used for the simulation resulting in circulation cells. The circulation cells are now less pronounced and there appears to be a global character to the liquid recirculation, although two smaller cells are still observed close to the bottom as can be seen in the velocity vector plot in Figure 3. The simulated time-averaged velocity and holdup profiles are much closer to the reported experimental results. The simulation results for this case is also averaged over the period from 25 to 100 seconds. The gas holdup profiles in the simulations with and without the circulation cells are shown in Figures 4 (a) and (b). As is often the case with simulations of bubble columns with CFDLIB, the holdup profiles are relatively uniform across the column although the centerline magnitudes are close to the reported values. The message then is that it is possible to change the results of simulation to closely match any observed experimental result, but what is not clear is the direction and magnitudes of the change required in the model parameters, since a consistent pattern has not been observed from the cases that have been attempted so far.

References

- Chen, J. J. J., Jamialahmadi, M. and Li, S. M., 1989, Effect of Liquid Depth on Circulation in Bubble Columns, Chem. Eng. Res. Des., Vol. 67, pp. 203-207.
- Lin, T. J., Reese, Hong, T., and Fan, L. S., 1996, Quantitative Analysis and Computation of Two-Dimensional Bubble Columns, AIChE J., Vol. 42, 2, pp 301-318.

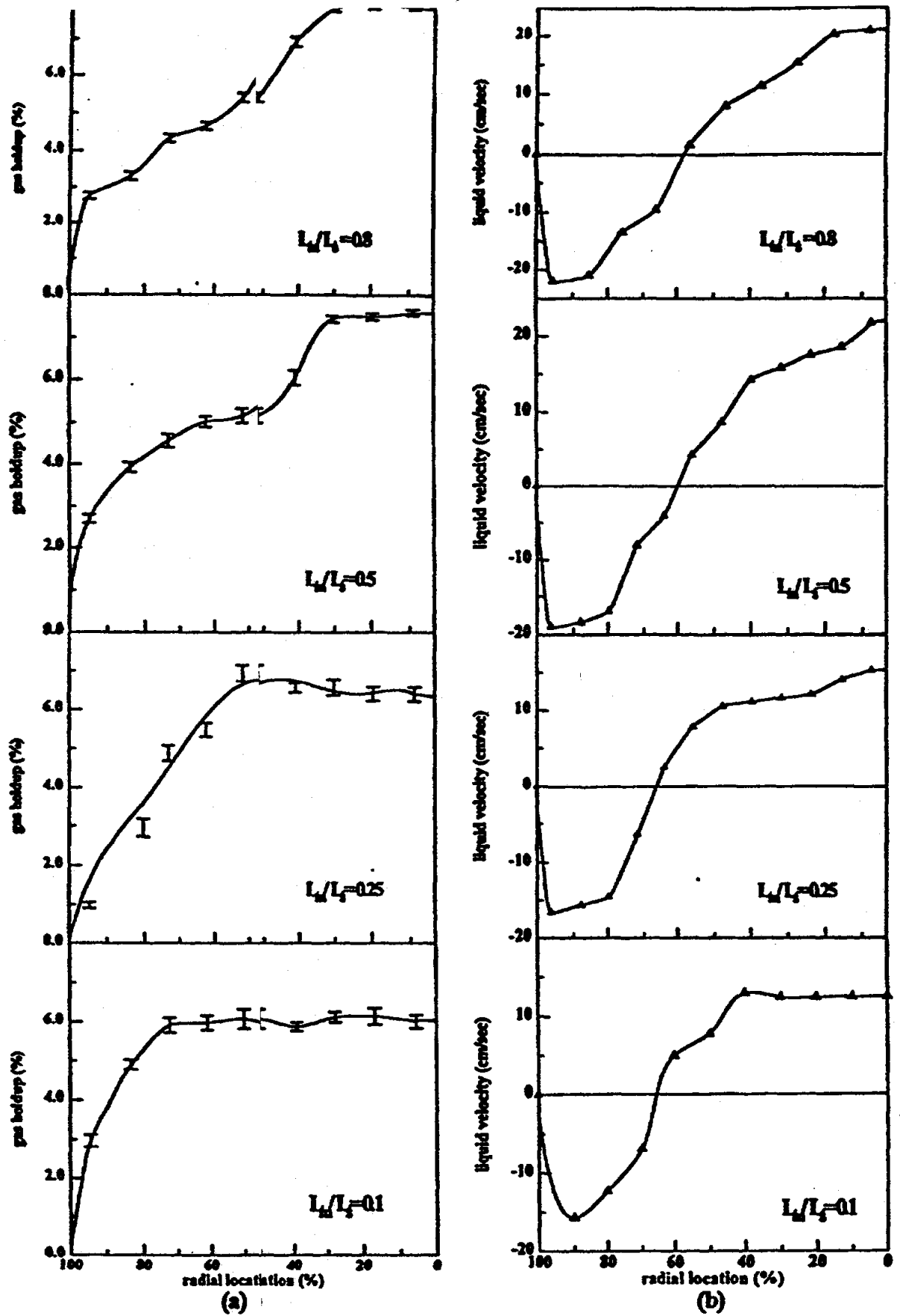


Figure 1. Radial gas holdup (a) and axial liquid velocity (b) distribution in 48.3 cm column at various axial locations $U_g = 3.34$ cm/s

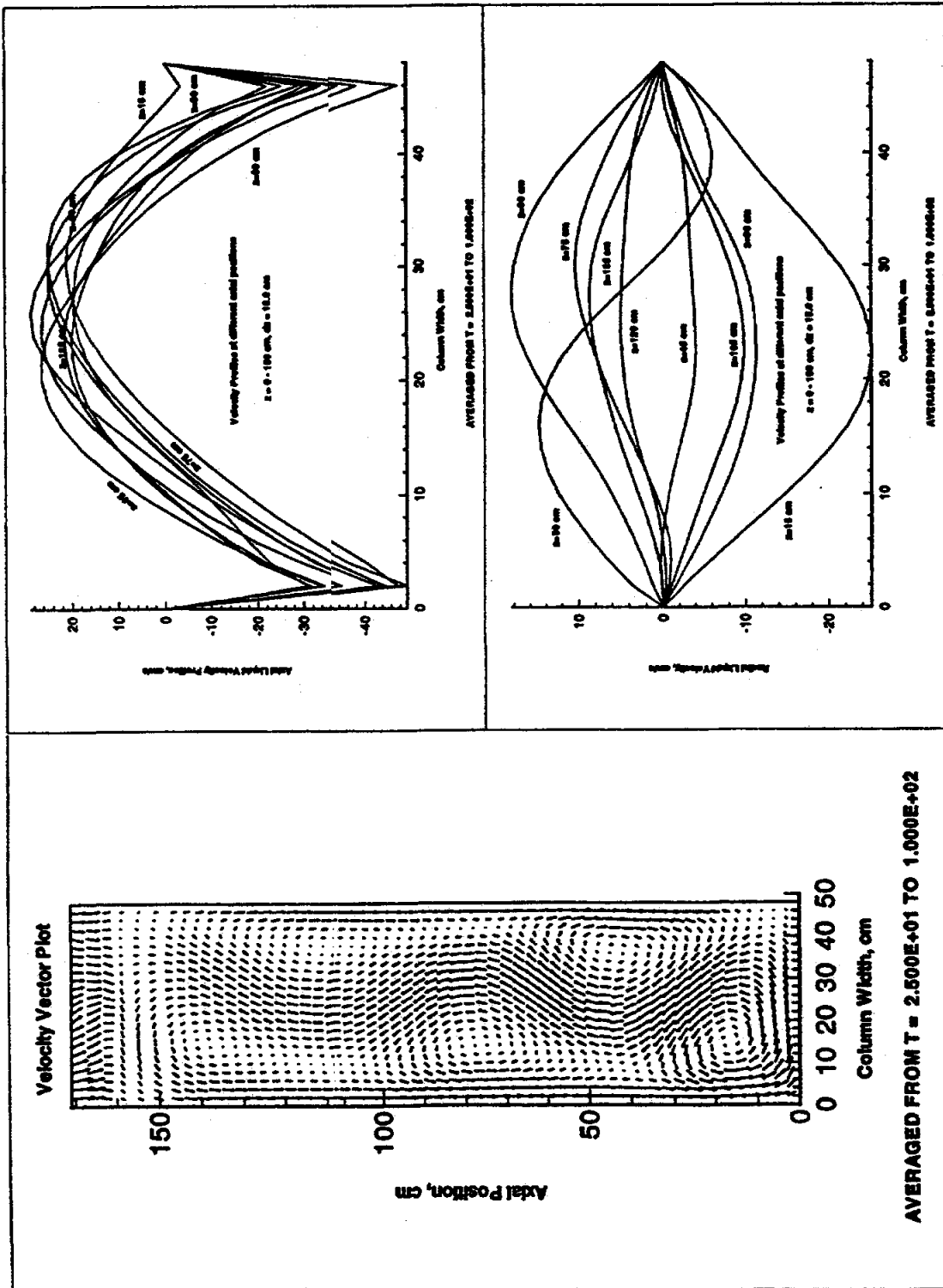


Figure 2. Simulation for the presence of circulation cells.

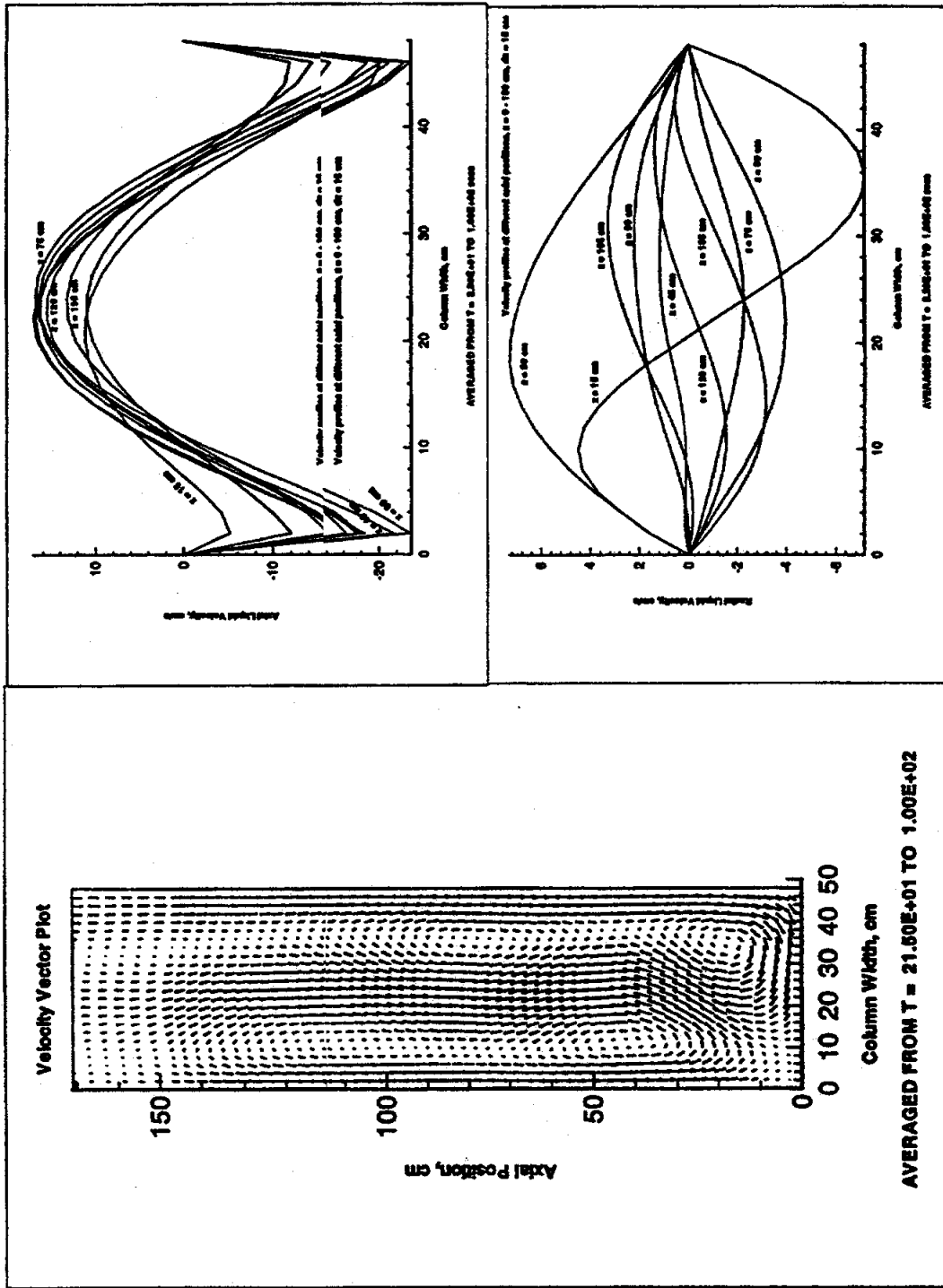


Figure 3. Simulation inhibiting the circulation cells.

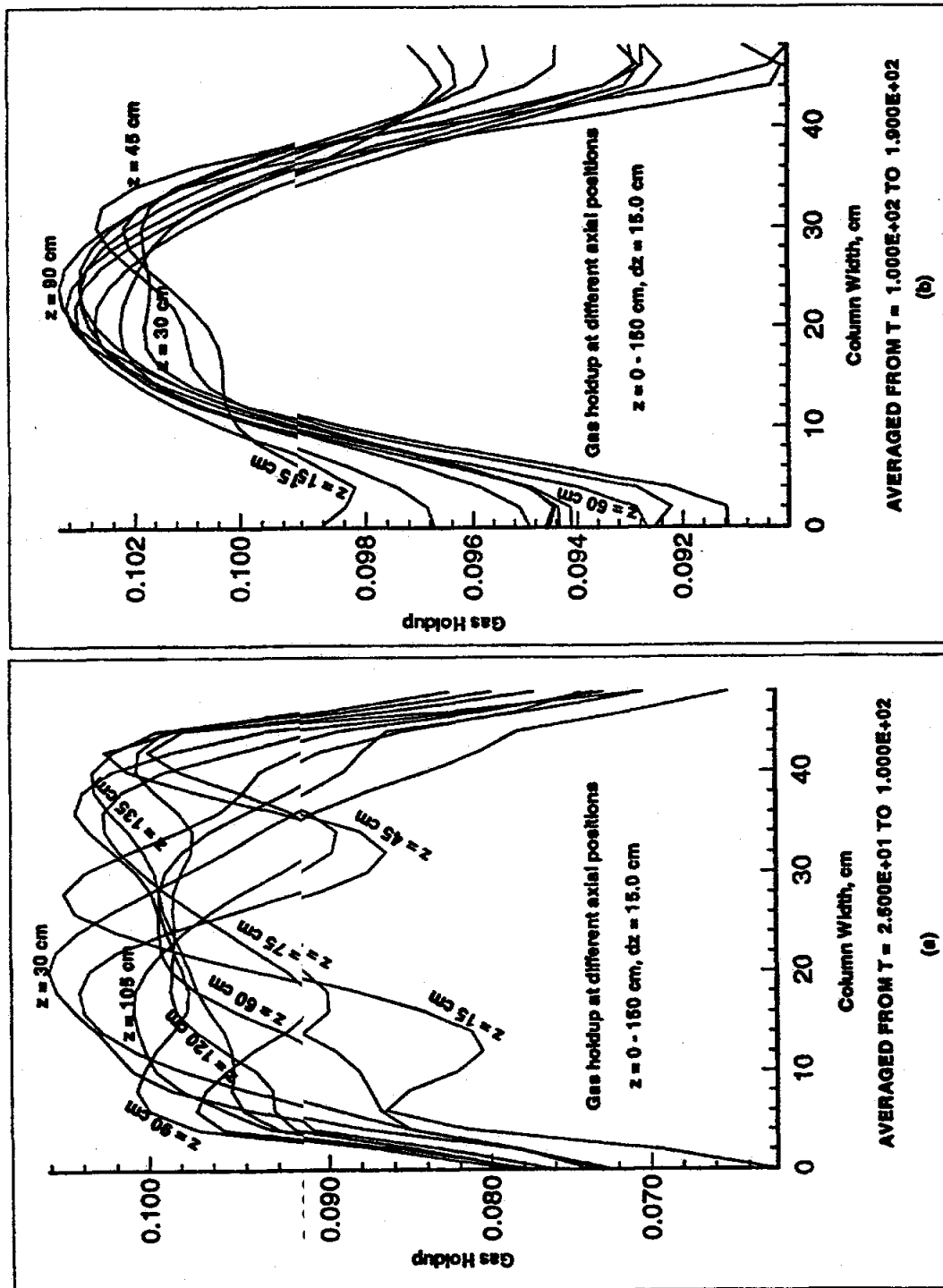


Figure 4. Gas holdup profiles with and without circulation cells.